Journal of Theoretical and Computational Chemistry
Vol. 12, No. 2 (2013) 1250108 (16 pages)

DOI: 10.1142/S0219633612501088

World Scientific
www.worldscientific.com

PLAUSIBLE BINDING MODE OF THE ACTIVE $\alpha 4\beta 1$ ANTAGONIST, MK-0617, DETERMINED BY DOCKING AND FREE ENERGY CALCULATIONS

C. MANUEL CARLEVARO[*,§], JOÃO HERMÍNIO MARTINS-DA-SILVA[†,¶], WILSON SAVINO[‡,‖] and ERNESTO RAÚL CAFFARENA[†,**]

[*]*Instituto de Física de Líquidos y Sistemas Biológicos (CONICET-UNLP)*
59 No 789, La Plata, Buenos Aires 1900, Argentina

[†]*Programa de Computação Científica (PROCC)*
Fundação Oswaldo Cruz, Ave. Brasil 4365 Manguinhos
21040-900, Rio de Janeiro, Brazil

[‡]*Laboratório de Pesquisas sobre o Timo*
Fundação Oswaldo Cruz, Ave. Brasil 4365 Manguinhos
21040-900, Rio de Janeiro, Brazil
[§]*manuel@iflysib.unlp.edu.ar*
[¶]*jhms@fiocruz.br*
[‖]*savino@fiocruz.br*
[**]*ernesto@fiocruz.br*

Received 18 April 2012
Accepted 30 August 2012
Published 21 December 2012

In the last years, the development of small molecule antagonists of VLA-4 for the treatment of diseases, where cell trafficking and activation are important, has increased considerably. Among them, the MK-0617 ligand has proven to be a highly potent and orally active $\alpha 4\beta 1$ antagonist. However, the binding mode of this ligand in the integrin binding site remains unknown. Herein we report a thermodynamic analysis of the interaction between MK-0617 (and one of its isomers) and the VLA-4 protein using molecular docking and the free energy perturbation calculations, based on a comparative model of the $\alpha 4\beta 1$ receptor. Initial complex coordinates were taken from molecular docking assays and submitted to alchemical transformations. Free energy of binding $\Delta\Delta G$ values, derived from experimental IC_{50} values, were taken as a parameter for determining the most likely binding mode. In addition, molecular dynamics simulations of these ligands within the $\alpha 4\beta 1$ binding site were carried out to elucidate the binding energy profile and identify the most significant residues. Our results indicate that MK-0617 fits within the binding site in a stretched conformation, pointing the carboxylate group towards the MIDAS ion. We observe that, despite the fact that the main contribution to the energetic binding process is due to the electrostatic ion contribution, the nonpolar contribution is not negligible. Additionally, a network of hydrogen bonds participate in stabilizing the ligand-receptor interaction.

Keywords: Integrin; molecular dynamics; binding mode.

1. Introduction

Integrins are heterodimers formed by two subunits, α and β, and their allowed combinations can result in 25 different classes. The existence of divalent cations (Mg^{+2}, Mn^{+2}) at the MIDAS (Metal Ion Depending Adhesion Site) active site is of central importance for the binding process. The fact that a coordinate bond between the MIDAS ion and a carboxylate group from the substrate has been found in all of the integrin-ligand interface centers reinforces its essential character, which represents a unique feature of integrins.[1] The elucidation of crystal structure of $\alpha V\beta 3$ largely contributed to the understanding of the binding of small protein ligands to integrins in general, regarding their high degree of the structural conservation.[2]

In particular, the $\alpha 4\beta 1$ integrin (VLA-4 or CD49d/CD29) is expressed by a variety of hemopoietic cell types including monocytes, T and B lymphocytes, basophils, and eosinophils. This integrin binds the alternatively spliced type III connecting segment (CS-1) of fibronectin, as well as the vascular cell adhesion molecule-1 (VCAM-1). From a therapeutic viewpoint, it is known that blocking $\alpha 4\beta 1$/VCAM-1 interaction relieves distinct autoimmune and inflammatory diseases, such as asthma, multiple sclerosis, rheumatoid arthritis, and type 1 diabetes.[3–6] This has generated significant interest in the development of small molecule antagonists of $\alpha 4\beta 1$ for the treatment of diseases where cell trafficking and activation are important. So far, the only $\alpha 4$ antagonist available on the market is natalizumab, a therapeutic monoclonal antibody directed against the $\alpha 4$ chain of both $\alpha 4\beta 1$ and $\alpha 4\beta 7$ integrins. Despite the existence of this novel antibody therapy, small molecule $\alpha 4$ antagonists are still a very attractive prospect, since the cost of goods of small molecules tends to be much lower than that of expensive antibody treatments.

Given the therapeutic relevance of these drugs, the number of new ligands has risen considerably in the last years.[7–21] Recently, Venkatraman *et al.* identified a family of prolyl-dipeptides containing secondary amines capable of acting as very potent oral antagonists against the $\alpha 4\beta 1$ integrin.[19] Among the compounds of the series, there was a specific drug named N-N-[(3-cyanobenzene) sulfonyl]-4(R)-(3,3-difluoropiperidin-1-yl)-(L)-prolyl-4-[(30,50-dichloro-isonicotinoyl) amino]-(L)-phenylalanine (MK-0617) with a IC_{50} value in the order of nanomolar magnitude. The authors suggested that the location of the fluorine group plays a critical role on the affinity, given that its isomer, with a 4,4-difluoropiperidine ring, was 7-fold less potent and exhibited a 2.5-fold lower receptor occupancy. However, detailed structural information about ligand receptor specific interactions of the MK-0617-compound with the $\alpha 4\beta 1$ integrin remains unknown.

It is well known that free energy perturbation (FEP) simulations, a technique able to calculate with high accuracy the relative free energy of binding between two structurally related ligands, is the most precise way to validate the more likely binding mode of a ligand in the protein binding site.[22] This prompted us to figure out the binding mode of this compound, in order to elucidate the suitable environment for binding of this class of compounds.

In this work, we performed docking and FEP transformations to determine the plausible binding mode of the MK-0617 molecule in the $\alpha 4\beta 1$ active site, based mainly on thermodynamic calculations. Also, a detailed structural study of the obtained binding modes is mandatory in order to obtain a more complete description, aiming to the construction of novel potent antagonists. In this line, molecular dynamics simulations helped us identify the residues in the MK-0617 vicinity that most contribute to the binding energy. We show herein that the thermodynamically most probable binding mode of MK-0617 fits within the binding site in a stretched conformation, pointing the carboxylate group towards the MIDAS ion. Despite the fact that the main contribution to the energetic binding process is due to the electrostatic ion contribution, the nonpolar contribution is not negligible.

The correlation of the experimentally determined binding affinities with the calculated binding energies led us to propose the binding mode with the carboxylate pointing toward MIDAS ion as plausible. Finally, the utilization of accurate simulation methods, namely, molecular docking and FEP, further verified our hypothesis.

2. Materials and Methods

In order to achieve computational reproduction of experimental binding affinities between the MK-0617 ligand and its analogue in the $\alpha 4\beta 1$ binding site, molecular docking, molecular dynamics simulations, and FEP methodologies were considered.

Spatial coordinates of MK-0617 ligand were built by using the Avogadro program.[a] The MKTOP program was applied to create topology files for the ligand with OPLS-AA force field parameters.[23,24] Atomic partial charges were retrieved from MMFF94 force field.[25]

The 3D structure of the $\alpha 4\beta 1$ headpiece was obtained by comparative modeling.[26] Briefly, we used the headpiece of $\alpha V\beta 3$ integrin (PDB code: 1L5G) in complex with Cilengitide (RGD ligand) as template to ensure the active conformation of the binding site for subsequent docking experiments. Atomic coordinates of the MIDAS motif divalent cations were merged into the binding site. The homology model thus obtained was then submitted to 1000 steps of steepest descent algorithm.[27] Labeling of amino acids of the receptor was taken from UNIPROT database under P13612 and P05556 codes for $\alpha 4$ and $\beta 1$ subunits, respectively.

Docking experiments were performed using Autodock-VINA software, an improved version of Autodock, which uses a gradient optimization method in its local optimization procedure.[28,29] About 25 runs were carried out to produce 500 solutions using different pseudorandom seeds. In each run, 200 binding modes are generated, out of which only the top 20, ranked by the VINA scoring function, are accessible to the user. The search was conducted in a cubic volume of $25 \times 25 \times 25$ Å^3, centered on the co-ordinates of the Mg^{+2} atom, with a value of 150 for exhaustiveness.

[a]Avogadro: An open-source molecular builder and visualization tool. Version 1.0.3. http://avogadro.openmolecules.net/

Results were clustered and ranked concerning geometric constraints and binding affinity, respectively. Three main groups of solutions (named models 1, 2, and 3, respectively) were regarded: (1) The best VINA solution, ranked according to the binding affinity, (2) solutions where the sulfone oxygen atoms were pointing to the central ion, and (3) solutions with the carboxyl oxygen atoms directed towards the MIDAS ion. Outcomes with their root mean square deviation (RMSD) differing in at most 2.5 Å were clustered in the same group and, the best representatives of each group were submitted to FEP transformations.

The accounting of the two last groups was based on previous reports that showed the relevance of the MIDAS motif in binding negatively charged groups.[30–32] Furthermore, Marinelli *et al.* have used the exclusion criterion based on structural information observed for RGD-ligand in the X-ray complex.[33] On these grounds, out of the 500 available solutions, we have only picked out those that presented any of their carbonyl or sulfone oxygen atoms pointing to the central MIDAS ion using a 7.0 Å cutoff.

Coordinates of the modeled molecular complex, $\alpha 4\beta 1$ integrin headpiece plus ligand, were immersed in a cubic TIP4P water box of dimension: $108.0 \times 88.0 \times 75.5\,\text{Å}^3$ and energy-minimized using the GROMACS software with periodic boundary conditions to fit the atomic positions to the OPLS-AA force field.[24,27,34] All interatomic bonds were constrained using the LINCS algorithm. Nonbonded interactions were taken into account using the 6-12 Lennard-Jones potential using a cutoff radius of 14 Å and PME electrostatic treatment with a 10 Å radius for coulomb interactions. Molecular dynamics simulations of the $\alpha 4\beta 1$ integrin headpiece in complex with ligands were performed in the NPT ensemble (300 K, 1 bar) using periodic boundary conditions with a 2 femtosecond (fs) timestep. All molecular dynamics simulations were performed with GROMACS.[27] The systems were simulated during 1 nanosecond (ns) restraining the protein co-ordinates to their initial positions, applying harmonic potential with spring constant $K = 50\,\text{kJ}/(\text{mol}\,\text{Å}^2)$ to stabilize water molecules around the protein. After solvent equilibration period, simulations evolved freely for more 1 ns, saving trajectories and velocities every 1 picosecond (ps) in order to analyze structural features.

Relative binding free energies were calculated by constructing a thermodynamic cycle. The principles behind this methodology have been reviewed elsewhere.[22] Briefly, the free energy change for the mutation of ligand A into B in a given medium is performed by a series of nonphysical, intermediate states along a connecting pathway. This pathway is characterized by a coupling parameter λ that allows the smooth transformation of the potential energy function $U(\lambda = 0)$, appropriate for ligand A, into a potential energy function suitable for ligand B, $U(\lambda = 1)$. N is the number of successive windows between A and B states, whereas R is the universal constant of gases and, T the absolute temperature:

$$\Delta G_{A\to B} = -\sum_{n=0}^{N-1} RT \ln \langle e^{-(U(\lambda_{n+1})-U(\lambda_n))/RT} \rangle_{(\lambda_n)}. \quad (1)$$

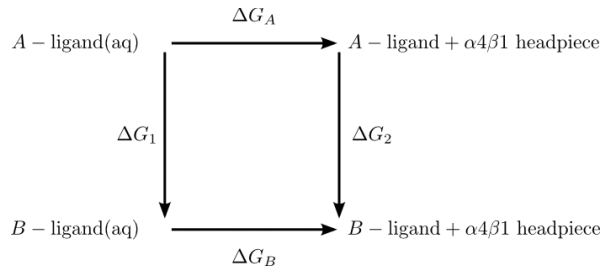

Fig. 1. Scheme depicting thermodynamic cycle for relative free energy of binding calculation. Alchemical transformations of the A-ligand into B-ligand were performed along the ΔG_1 and ΔG_2 pathways.

Subsequently, FEP calculations were carried out according to the classical thermodynamic cycle, to determine the relationship between binding constants ratio between the ligand containing the 4,4-difluoropiperdine group and MK-0617 (henceforth A and B, respectively) and relative free energy of binding values, as seen in Fig. 1.

The final 1 ns configuration that resulted from MD equilibration period was regarded as the starting point for FEP transformations. Along these paths, the two fluorine atoms belonging to the piperdine ring, originally in (4,4) position were smoothly displaced to position (3,3), in both aqueous solution and within the binding site.

The atomic parameters were perturbed in forward and backward directions (double-wide sampling) comprising a total number of 17 windows equally spaced in steps of $\Delta\lambda = 0.0625$, allowing an estimation of the hysteresis and the Zwanzig equation was used to calculate the free energies $\Delta G(\lambda + \Delta\lambda)$ and $\Delta G(\lambda - \Delta\lambda)$.[35] A linear coupling parameter λ was applied and no atoms were annihilated or created. The system evolved 500 ps per window, estimating 100 ps for system adaptation to the new value of λ, and 400 ps for averaging. The mean value of ΔG, derived from forward and backward runs, was taken as the representative value for each window with the standard deviation as a lower estimation of the error.

Finally, we carried out MD simulations of A and B isomers within the $\alpha4\beta1$ binding site, taking as initial co-ordinates those resulting from the final configurations of extreme states, A ($\lambda = 0$) and B ($\lambda = 1$). Both systems evolved freely for 15 ns. Trajectories and velocities were stored every 2 ps to analyze structural features. All calculations were carried out on a Intel(R) Core(TM) i7 CPU (2.67 GHz) machine.

3. Results

3.1. *Docking*

The MK-0617 isomer, containing the 4,4-difluoropiperidine group, was docked at the interface of α and β subunits of the $\alpha4\beta1$ integrin headpiece. An exhaustive docking

search was conducted to determine a suitable set of co-ordinates as starting points for FEP transformations. The 500 solutions were clustered and sorted out in three main groups as described in material and methods section resulting in 22 different groups, four of them with less than four solutions.

The cluster 1, named best solution cluster, grouped 194 solutions (representing 38.8% of the total) with average affinity and minimum values equal to -41.50 ± 1.72 and -43.51 kJ/mol, respectively. Using a 5 Å cutoff, we found that the closest amino acids from the ligand were: Tyr220, Trp221, Lys246, Phe247, Gly248, Tyr250, Gln274, Gln277 for $\alpha 4$ unit and Asp246, Ser247, Pro248, Gly281, Phe282, Phe341, and Val344 for $\beta 1$ unit. Also, in this particular conformation fluorine atoms were near Phe282 and Val344 of $\beta 1$ subunit.

Solutions where the sulfone atoms were pointing to the central ion were spread among several clusters. Anyhow, the solution with sulfone oxygen atoms located at distances of 7.77 Å and 6.54 Å, respectively from MIDAS ion was chosen as representative of cluster 2, with an affinity value of -40.60 ± 0.50 kJ/mol. Neighboring amino acids were: Glu157, Lys159, Lys189, Lys190, Phe195, Tyr220 for $\alpha 4$ chain and Tyr153, Ser154, Ser197, Pro200, Leu203, Cys207, Thr208, Ser209, Gln211, Asn244, Leu245 for $\beta 1$, up to a cutoff of 5 Å.

In cluster 3, 44 solutions (8.82%), with the carboxyl group pointed to the MIDAS ion, were assembled, with mean affinity value of -39.75 ± 0.79 kJ/mol and minimum of -42.26 kJ/mol. The average distances from O1 and O2 of the acidic group to the MIDAS ion were 6.65 ± 0.85 Å and 6.99 ± 0.80 Å, respectively. The set of neighboring amino acids, up to 4 Å from the ligand, was: Tyr220, Trp221, Lys246, Phe247, Gly248, Tyr250, Gln274, Gln277 for β-propeller and Asp246, Ser247, Pro248, Gly281, Phe282, Phe341, Val344 for $\beta 1$. For this solution fluorine atoms were in the proximity of: Ser197, Leu203, Pro208, Cys207, Thr208, Gly243, Asn244 of the β subunit.

The best candidates (the complexes with minimum affinity values in each cluster) from these three particular groups were chosen for FEP calculations.

3.2. *FEP*

The molecular docking process allowed us to determine a set of plausible binding modes for the ligands, as well as the energetic background of the selectivity phenomenon. However, these results must still be corroborated with experimental data by means of alternative methodologies such as molecular-mechanics based methods. Thus, we decided to study the binding of MK-0617 ligand and its analogue by FEP transformations. The conversion of 4,4-difluoropiperdine (compound A) into 3,3-difluoropiperdine (compound B) is within the method limits and three docked configurations, named models 1, 2, and 3, were submitted to alchemical transformations by transforming isomer A into B, according to the thermodynamic cycle (see Fig. 2). A more detailed explanation of these configurations is given in the material and methods section.

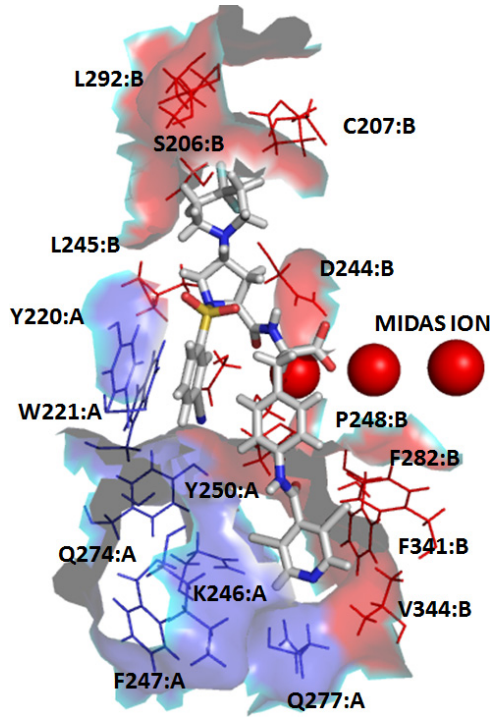

Fig. 2. (Color online) Residues in the vicinity of MK-0617 isomer, as defined by the model 3 solution obtained by Vina Autodock program. The A and B labels indicate the $\alpha 4$ (blue) and $\beta 1$ (red) integrin chains.

The $\Delta G_{\text{binding}}$ was calculated as $\Delta\Delta G_{\text{binding}}(A \to B) = \Delta G_{\text{bound}}(A \to B) - \Delta G_{\text{free}}(A \to B)$. The computed difference in free energy of binding of A and B, based on the experimental-reference data obtained from Venkatraman *et al.*, was in agreement with experimental results, i.e. a $\Delta\Delta G$ value of $-2.04 \pm 1.54\,\text{kJ/mol}$ (experimental $-4.97\,\text{kJ/mol}$), in favor of isomer B to A for model 3.[19] FEP calculations also showed a better approximation to the experimental value, with an absolute error less than $3\,\text{kJ/mol}$, whereas models 1 and 2 resulted in $11.12 \pm 2.84\,\text{kJ/mol}$ and $-0.87 \pm 1.26\,\text{kJ/mol}$, respectively. This suggests that the best docked solution does not correspond to the right binding mode of MK-0617 ligand and that positioning of sulfone towards MIDAS ion also does no result in a propitious environment for binding, since $\Delta\Delta G$ values approach zero.

The error associated to the calculations is typically estimated as the difference between the pseudoindependent "forward" and "backward" pathways for a single run. As forward-and-backward results are not exactly the same, their difference gives a rudimentary lower bound on the inherent error. To circumvent this limitation, the statistically-based errors were calculated using a block averaging approach, which essentially places groups of consecutive system configurations into a single block. The average of each block was determined and then used as the single observation for

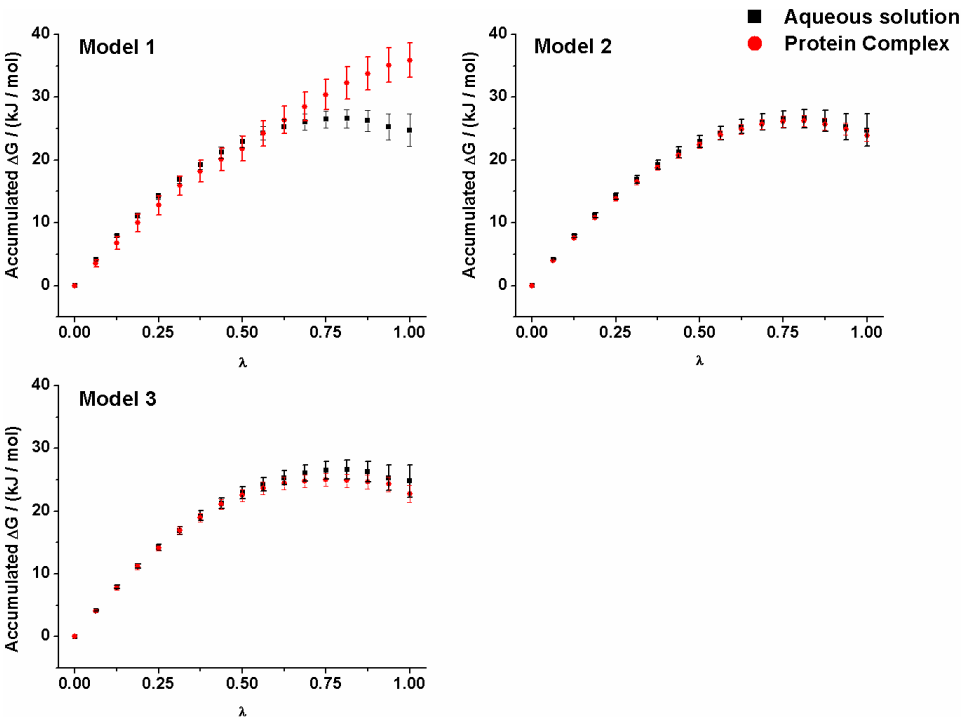

Fig. 3. Free-energy curves obtained in water, and the protein for models 1, 2, and 3. $\Delta\Delta G$ values were calculated as the subtraction between the final values ($\lambda = 1$) for the solution and complex simulations. Error bars were calculated by applying the block average method.

that block. Afterwards, the variance for the series of block values was calculated. The estimated relative binding free energies for the three models are shown in Fig. 3.

3.3. *Interaction energy profile*

Interaction energies between MK-0617 and receptor were analyzed to identify the key residues for binding, from molecular dynamics simulations. The average interaction energies for the $\alpha 4\beta 1$ residues that significantly contributed to the binding free energy are shown in Table 1.

Around 10 out of the 16 amino acids that account for energetic contributions higher than 4.184 kJ/mol (1 kcal/mol) belong to the β subunit, totalizing 68% of the total contribution. The amino acid residues Y220 of the α subunit, and, N244, L245, S247, and E340 of the β subunit were here found to have either highly favorable electrostatic or van der Waals interactions with the compound, indicating their importance for tight binding. Residues Y220:A, N244:B, L245:B, S247:B, and E340:B contributed with more than 20 kJ/mol each. The average electrostatic and van der Waals interaction energies for the residues that most contribute to the binding free energy are shown in Fig. 4.

Table 1. Interaction energy profile for the MK0617 ligand and its surrounding neighbors within a 5 Å cutoff.

Residue	Electrostatic	Lennard-Jones	Total
S197:A	-7.48 ± 8.90	-3.2 ± 3.49	-10.70 ± 9.56
Y220:A	-11.78 ± 15.48	-23.73 ± 4.64	-35.50 ± 16.16
W221:A	-0.53 ± 1.05	-8.61 ± 2.19	-9.15 ± 2.43
V245:A	1.50 ± 2.93	-8.55 ± 5.88	-7.05 ± 6.57
K246:A	-4.19 ± 4.05	-13.56 ± 4.24	-17.75 ± 5.86
F247:A	-3.67 ± 3.35	-11.11 ± 4.67	-14.77 ± 5.74
Y153:B	-3.17 ± 1.47	-13.32 ± 3.73	-16.50 ± 4.01
S154:B	0.60 ± 4.31	-6.00 ± 2.43	-5.40 ± 4.95
S197:B	-2.82 ± 6.07	-2.24 ± 1.29	-5.06 ± 6.20
G243:B	-2.09 ± 2.07	-4.33 ± 1.56	-6.92 ± 2.60
N244:B	-2.62 ± 5.62	-20.21 ± 3.69	-22.82 ± 6.72
L245:B	-1.19 ± 2.56	-24.79 ± 5.03	-25.98 ± 5.64
D246:B	-4.67 ± 3.96	-11.65 ± 2.56	-16.32 ± 4.71
S247:B	-2.93 ± 10.93	-19.84 ± 3.62	-22.77 ± 11.52
E340:B	-47.58 ± 35.87	-14.54 ± 5.82	-62.12 ± 36.34
F341:B	-2.59 ± 1.59	-14.06 ± 3.11	-16.65 ± 3.49
MIDAS ION	-71.56 ± 13.45	-0.68 ± 0.13	-72.25 ± 13.45

Note: Units are given in kJ/mol.

The most important contribution to binding comes from the electrostatic term due to the proximity between the carboxylate group and the MIDAS ion, yielding a strong binding interaction of -71.56 ± 13.45 kJ/mol. This evidence supports the fact that the MIDAS ion plays a crucial role in the binding process between integrins and corresponding ligands.

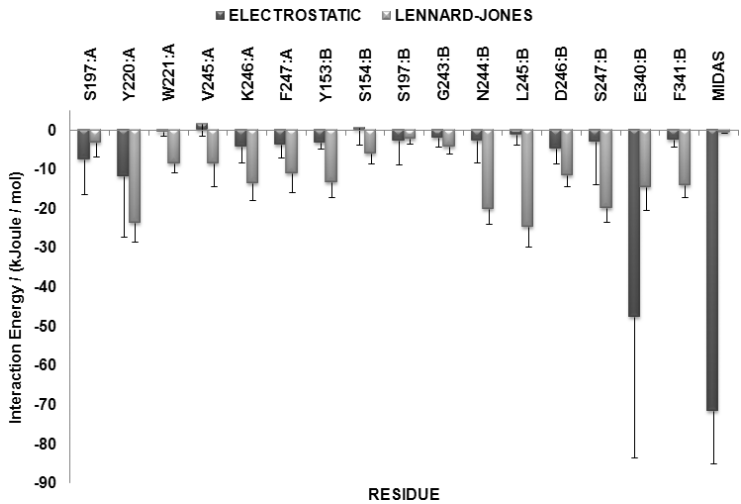

Fig. 4. Bar representation of electrostatic (black) and Lennard-Jones (gray) average ligand-residue interaction energies for the residues that most contribute to the ligand-surrounding (up to 5 Å) after 15 ns simulation of MK-0617 binding. The average interaction energies are given in kJ/mol, and the corresponding standard deviations are shown.

Another significant contribution arises from nonpolar terms of the force field equation. In particular, residues Y220:A, L245:B, and S247:B account for the largest contribution to the ligand-residue interaction energies with averages equal to -23.85 ± 4.6, -24.68 ± 5.02, and -19.66 ± 3.77 kJ/mol, respectively. This shows that binding is clearly favored by van der Waals interactions with these residues.

As far as concerns the electrostatic contributions for neighbor residues, these remained below 10 kJ/mol, except Y220:A and E340:B, with values of -11.72 ± 2.1 kJ/mol and -11.4 ± 8.79 kJ/mol, respectively. Furthermore, the standard deviations in ligand-residue electrostatic energies are larger than the interaction energies obtained for the Lennard-Jones contribution. In particular, S197:A, Y220:A, S2475:B, and E340:B have deviations over than 8 kJ/mol, whereas all nonpolar deviations do not exceed 5 kJ/mol.

Curiously, E340:B presented a high electrostatic contribution to the interaction energy, with the largest deviation. Structurally, this energetic contribution can be traced back to the strength of the hydrogen bond between the ligand and the E340:B backbone carbonyl, along with the side chain oxygen atoms. The high deviation is due to the intermittent repulsion between negatively charged nitrogen atoms of the ligand and the oxygen atoms belonging to the E340:B residue. From a sterical viewpoint, the volumetric distribution of important amino acids for binding is equally balanced between α and β subunits. The benzonitrile ring, that interacts with a highly hydrophobic pocket determined by Y220:A, W221:A, and Y250:A of the $\alpha 4$ subunit, is supported mainly by π-stacking and T-stacking interactions between aromatic rings. V245:A, K246:A, and F247:A also appear as important residues in the $\alpha 4$ subunit, interacting mainly with the 3,5-dichloro pyridin ring. This specific group also makes contact with E340:B.

As far as fluorine atoms energy contribution concerns, it is noteworthy that the major contribution comes from nonpolar interactions, given that electrostatic values were not lower than -5 kJ/mol. van der Waals interaction for the MK-0617 ligand better accounts for binding than its isomer, with specific important contributions from N244:B, S152:B, and Y153:B residues from the $\beta 1$ subunit. Figure 5 shows

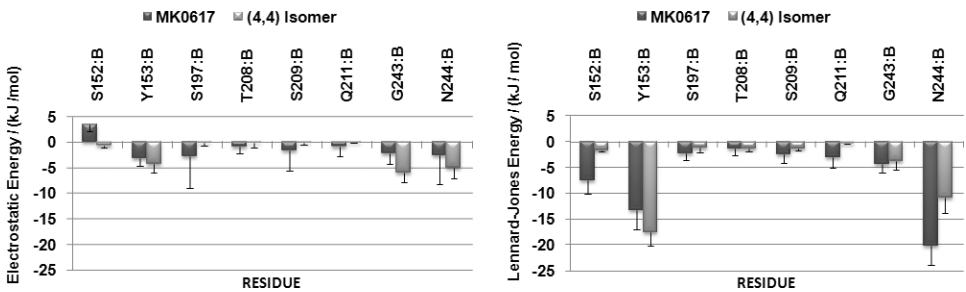

Fig. 5. (Color online) Bar representation of electrostatic (black) and Lennard-Jones (gray) interactions between MK-0617 (and its isomer) and the residues in the vicinity of fluorine atoms (up to 6 Å). The average interaction energies are given in kJ/mol, and the corresponding standard deviations are shown. The (3,3) difluoropiperdine and the (4,4) difluoropiperdine labels indicate the position of fluorine atoms in MK-0617 and its isomer, respectively.

energetic contribution from residues up to 6 Å in the surrounding of fluorine atoms. Total interaction energies between these residues and MK-0617 and the (4,4) isomer are −64.78 kJ/mol and −53.76 kJ/mol, respectively.

The analysis of the figure reveals that the relocation of this group, from (4,4) to (3,3), results in a gain of about 10 kJ/mol, favoring the interaction of MK-0617 with the $\beta 1$ subunit.

3.4. *Structural analysis*

For a more accurate description of ligand-protein interaction and its effects, structural and thermodynamic analyzes provide complementary information and both are needed. Thus, a detailed analysis of the most significant specific interactions between the $\alpha 4\beta 1$ headpiece and MK-0617 ligand is given below.

An inspection of the intermediate structure trajectories of the mutation showed a gradual approaching of the carboxyl group of the ligand to the MIDAS ion, starting at 6.6 ± 0.4 Å for $\lambda = 0$ and ending at 4.7 ± 0.3 Å for $\lambda = 1$. The difluoropiperdine group was steadily changing its orientation in the binding site, achieving its final conformation with the fluorine atoms more exposed to the solvent. Analysis of the fluorine radial distribution functions revealed that the MK-0617 ligand presents a higher probability of finding a water molecule at close distances, when compared with the (4,4) isomer (Fig. 6(a)).

The calculated B-factors, shown in Fig. 6(b), illustrate how the ligand binding influences the positional fluctuations of the protein neighboring residues. B-factors are comparable for both ligands, except for the residues V245:A, K246:A, which interact with the benzonitrile ring, and E340:B that interacts with the 3,5-dichloro pyridin ring. Average RMSD values for the MK-0617 and its isomer were 1.26 ± 0.16 Å and 2.31 ± 0.34 Å, respectively, suggesting a slightly better stability for MK-0617 in the binding site.

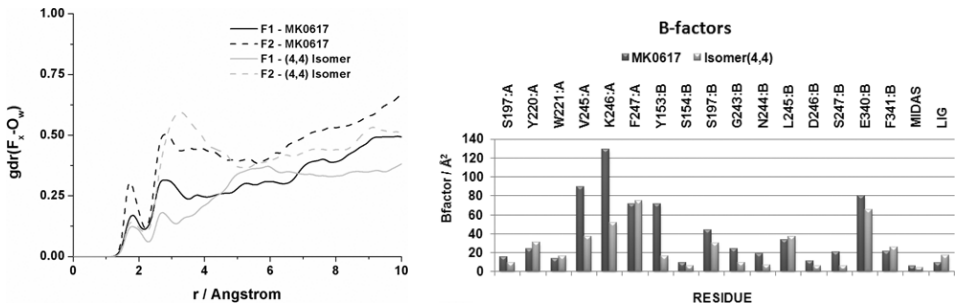

(a) (b)

Fig. 6. Panel (a) depicts the radial distribution functions for fluorine atoms of both MK-0617 ligand (straight and dashed black lines) and (4,4) isomer (straight and dashed gray lines). These correlation functions stabilize at unitary value at long distances (∼ 30 Å). Panel (b) shows calculated B-factors for the $\alpha 4\beta 1$ residues in the vicinity of the MK-0617 ligand.

Finally, a set of hydrogen bonds also participates in the maintenance of MK-0617 within the intersection between the two subunits. Four main hydrogen bonds help to stabilize the MK-0617 within the $\alpha 4\beta 1$ headpiece, three of them acting as acceptors and only one as donor. In particular, the hydrogen bonds formed with S154 and S247 and the oxygen atom of the MK-0617 carbonyl and carboxyl groups, respectively, were constantly held. The intermittent hydrogen bond interaction between the amide group of MK-0617 and the OE1 oxygen atom of E340:B is responsible for the high deviation of the electrostatic energy contribution of this particular residue. Other less significant hydrogen bonds form sporadically between the ligand and receptor.

Despite the high electronegative character of the fluorine atoms, they are not good hydrogen bond formers, and do not form relevant specific bonds with the protein. Radial distribution functions of fluorine atoms showed that when they are located at the 3,3 position, they present a slightly more hydrated shell, since these atoms remain more exposed to the solvent. The time evolution of the main H-bonds is shown in Fig. 7.

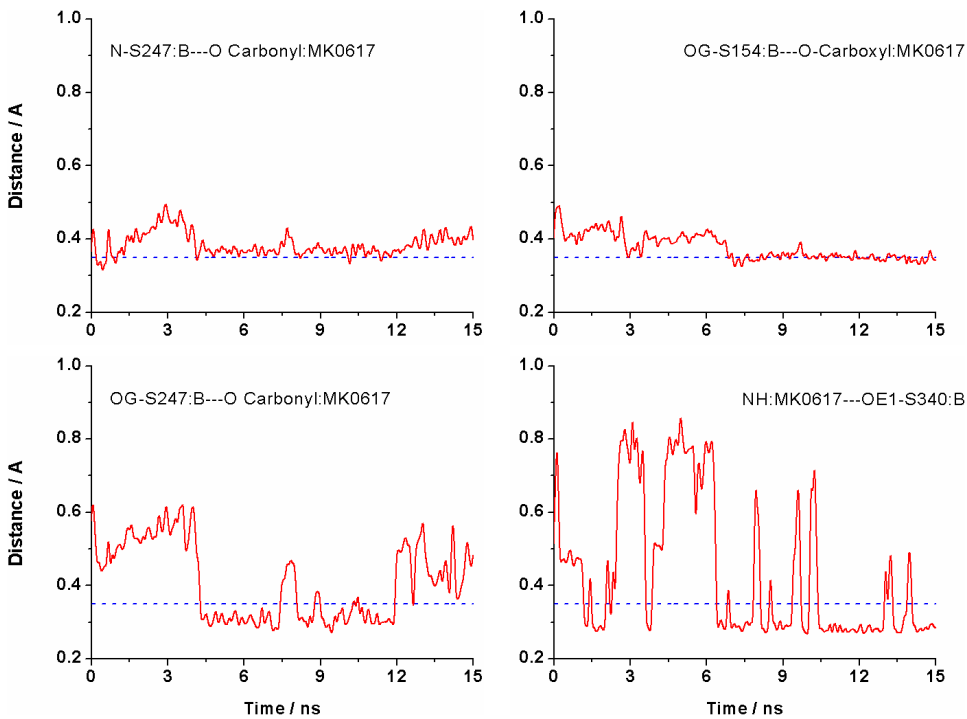

Fig. 7. Time evolution of main hydrogen bonds formed between the MK-0617 compound and the $\alpha 4\beta 1$ integrin over 15 ns MD simulation. The constant line indicates the upper limit for an hydrogen bond to be considered as such. The A-H—O angle must be between 145° and 225°, where A and O are the electronegative atoms involved in the interaction.

4. Discussion

In the present study we applied computational techniques, docking, scoring, and MD simulations in combination with the FEP method in order to determine the most likely binding mode of MK-0617 ligand in the binding site of the $\alpha 4\beta 1$ integrin. The calculations illustrate that, although MD simulations are computationally expensive, the FEP method provides a useful approach for obtaining accurate predictions of protein-ligand binding free energies. The degree of agreement with experimental data suggests that the MK-0617 compound locates within the binding site in an extended conformation, with the carboxylate oxygen atoms pointing to the MIDAS ion. This observation reinforces the previous finding that the predominance of an extended conformation in solution is a potential feature that would help in the binding process, resulting in an enhanced affinity of the prototype compound for the $\alpha 4\beta 1$ integrin.[26]

Molecular dynamics trajectories were analyzed in terms of ligand conformations, energy profile, hydrogen bond interactions between ligand and amino acid residues in the active site, and in terms of flexibility.

The protein-antagonist interactions were analyzed in detail, finding that the binding free energy of this ligand can be described using only a few specific receptor interactions. The major factor responsible for the correct ligand binding in the binding site remains the interaction between the ligand carboxylic group and MIDAS ion. Nevertheless, nonpolar interactions participate substantially in maintaining the ligand well fitted within the binding site. As far as concerns the position of the fluorine atoms in the piperdine ring, its location at the 3.3 position favors the interaction of ligand with the $\beta 1$ subunit, with predominant nonpolar interactions, additionally slightly exposed to solvent.

The repositioning of fluorine atoms, along with a higher interaction with solvent, result in an enthalpic gain for MK0617, which remains more stable within the cleft than its isomer. Finally, a network of H-bonds also participate in the maintenance of the ligand within the integrin binding site.

The identification of these main interactions can provide important clues for further optimization of ligand affinity as well as contribute in the design of inhibitors that are less susceptible to mutations. Also, such overall description of the main residues that contribute to the binding suggest that efficient models for estimating ΔG variation may be based mostly on monitoring a subset of the ligand-residue interactions. By introducing empirical scaling factors for each interaction energy, multivariate analysis can be used to identify the energetic contributions from the binding site that best reproduce the experimental data. The parameterized model can then be applied in scoring and lead optimization of inhibitors of unknown activity.

Identification of the hotspots in the $\alpha 4\beta 1$ integrin allows the possibility of creating an energy scoring function to select the best candidates of MK-0617 derivatives in a fast and nonexpensive way.

In conclusion, the results presented herein are in agreement with the $\Delta\Delta G$ calculated from experimental IC_{50} values, and show the effectiveness of thermodynamics-based

combined computational methodologies, not only for the development and characterization of new VLA-4 inhibitors, but also for other drugs that act through protein−protein interactions.

Acknowledgments

The authors are indebted to Andrés McCarthy for his comments and suggestions. This work was supported by PROCC/FIOCRUZ, CNPq, and Faperj, Brazil. C.M. Carlevaro is a member of CONICET, Argentina.

References

1. Takagi J, Structural basis for ligand recognition by integrins, *Curr Opin Cell Biol* **19**:557−564, 2007.
2. Xiong JP, Stehle T, Zhang R, Joachimiak A, Frech M, Simon LG, Arnaout MA, Crystal structure of the extracellular segment of integrin $\alpha V\beta 3$ in complex with an Arg-Gly-Asp ligand, *Science* **296**:151−155, 2002.
3. Abraham WM, Sielczak MW, Ahmed A, Cortes A, Lauredo IT, Kim J, Pepinsky B, Benjamin CD, Leone DR, Lobb RR, Alpha(4)-integrins mediate antigen-induced late bronchial responses and prolonged airway hyperresponsiveness in sheep, *J Clin Invest* **93**:776−787, 1994.
4. Hafler DA, Multiple sclerosis, *J Clin Invest* **113**:788−794, 2004.
5. Seiffge D, Protective effects of monoclonal antibody to VLA-4 on leukocyte adhesion and course of disease in adjuvant arthritis in rats, *J Rheumatol* **23**:2086−2091, 1996.
6. Yang XD, Karin N, Tisch R, Steinman L, Mcdevitt HO, Inhibition of insulitis and prevention of diabetes in nonobese diabetic mice by blocking L-selectin and very late antigen-4 adhesion receptors, *Proc Natl Acad Sci USA* **90**:10494−10498, 1993.
7. Chang LL, Truong Q, Doss GA, MacCoss M, Lyons K, McCauley E, Mumford R, Vincent S, Schmidt JA, Hagmann W, Highly constrained bicyclic VLA-4 antagonists, *Bioorg Med Chem Lett* **17**:597−601, 2007.
8. Chang LL, Yang GX, McCauley E, Mumford RA, Schmidt JA, Hagmann WK, Constraining the amide bond in N-Sulfonylated dipeptide VLA-4 antagonists, *Bioorg Med Chem Lett* **18**:1688−1691, 2008.
9. Chiba J, Iimura S, Yoneda Y, Sugimoto Y, Horiuchi T, Muro F, Ochiai Y, Ogasawara T, Tsubokawa M, Iigou Y, Takayama G, Taira T, Takata Y, Yokoyama M, Takashi T, Nakayama A, Machinaga N, 4-(pyrrolidinyl)methoxybenzoic acid derivatives as a potent, orally active VLA-4 antagonist, *Chem Pharm Bull* **54**:1515−1529, 2006.
10. Chiba J, Iimura S, Yoneda Y, Watanabe T, Muro F, Tsubokawa M, Iigou Y, Satoh A, Takayama G, Yokoyama M, Takashi T, Nakayama A, Machinaga N, Synthesis and biological evaluation of benzoic acid derivatives as potent, orally active VLA-4 antagonists, *Bioorg Med Chem* **15**:1679−1693, 2007.
11. Chiba J, Machinaga N, Takashi T, Ejima A, Takayama G, Yokoyama M, Nakayama A, Baldwin JJ, McDonald E, Saionz KW, Swanson R, Hussain Z, Wong A, Identified a morpholinyl-4-piperidinylacetic acid derivative as a potent oral active VLA-4 antagonist, *Bioorg Med Chem Lett* **15**:41−45, 2005.
12. Chiba J, Takayama G, Takashi T, Yokoyama M, Nakayama A, Baldwin JJ, McDonald E, Moriarty KJ, Sarko CR, Saionz KW, Swanson R, Hussain Z, Wong A, Machinaga N, Synthesis, biological evaluation, and pharmacokinetic study of prolyl-1-piperazinylacetic

acid and prolyl-4-piperidinylacetic acid derivatives as VLA-4 antagonists, *Bioorg Med Chem* **14**:2725−2746, 2006.
13. Gong Y, Barbay JK, Kimball ES, Santulli RJ, Fisher MC, Dyatkin AB, Miskowski TA, Hornby PJ, He W, Synthesis and SAR of pyridazinone-substituted phenylalanine amide α_4 integrin antagonists, *Bioorg Med Chem Lett* **18**:1331−1335, 2008.
14. Kamenecka TM, Park YJ, Lin LS, de Laszlo S, McCauley ED, van Riper G, Egger L, Kidambi U, Mumford RA, Tong S, Tang W, Colletti A, Teffera Y, Stearns R, MacCoss M, Schmidt JA, Hagmann WK, Amidines as amide bond replacements in VLA-4 antagonists, *Bioorg Med Chem Lett* **14**:2323−2326, 2004.
15. Lassoie MA, Broeders F, Collart P, Defrere L, de Laveleye-Defais F, Demaude T, Gassama A, Guillaumet G, Hayez JC, Kiss L, Knerr L, Nicolas JM, Norsikian S, Quéré L, Routier A, Verbois V, Provins L, 2,6-Quinolinyl derivatives as potent VLA-4 antagonists, *Bioorg Med Chem Lett* **17**:142−146, 2007.
16. Phillips DJ, Davenport RJ, Demaude TA, Galleway FP, Jones MW, Knerr L, Perry BG, Ratcliffe AJ, Imidazopyridines as VLA-4 integrin antagonists, *J Bioorg Med Chem Lett* **18**:4146−4149, 2008.
17. Reger TS, Zunic J, Stock N, Wang B, Smith ND, Munoz B, Green MD, Gardner MF, James JP, Chen W, Alves K, Si Q, Treonze KM, Lingham RB, Mumford RA, Heterocycle-substituted proline dipeptides as potent VLA-4 antagonists, *Bioorg Med Chem Lett* **20**:1173−1176, 2010.
18. Saku O, Ohta K, Arai E, Nomoto Y, Miura H, Nakamura H, Fuse E, Nakasato Y, Synthetic study of VLA-4/VCAM-1 inhibitors: Synthesis and structure-activity relationship of piperazinylphenylalanine derivatives, *Bioorg Med Chem Lett* **18**:1053−1057, 2008.
19. Venkatraman S, Lebsack AD, Alves K, Gardner MF, James J, Lingham RB, Maniar S, Mumford RA, Si Q, Stock N, Treonze KM, Wang B, Zunic J, Munoz B, Discovery of N-N-[(3-cyanobenzene)sulfonyl]-4(R)-(3,3-difluoropiperidin-1-yl)-(L)-prolyl-4-[(3′,5′-dichloroisonicotinoyl) amino]-(L)-phenylalanine (MK-0617), a highly potent and orally active VLA-4 antagonist, *Bioorg Med Chem Lett* **19**:5803−5806, 2009.
20. Witherington J, Vincent BA, Gaiba A, Green PM, Naylor A, Parr N, Smith DG, Takle AK, Ward RW, Pyridone derivatives as potent and selective VLA-4 integrin antagonists, *Bioorg Med Chem Lett* **16**:2256−2259, 2006.
21. Dyatkin AB, Gong Y, Miskowski TA, Kimball ES, Prouty SM, Fisher MC, Santulli RJ, Schneider CR, Wallace NH, Hornby PJ, Diamond C, Kinney WA, Maryanoff BE, Damiano BP, He W, Aza-bicyclic amino acid carboxamides as alpha(4)beta(1)/alpha(4)beta(7) integrin receptor antagonists, *Bioorg Med Chem Lett* **13**:6693−6702, 2005.
22. Kollman P, Free-energy calculations — Applications to chemical and biochemical phenomena, *Chem Rev* **93**:2395−2417, 1993.
23. Ribeiro AAST, Horta BAC, de Alencastro RB, MKTOP: A program for automatic construction of molecular topologies, *J Braz Chem Soc* **19**:1433−1435, 2008.
24. Jorgensen WL, Maxwell DS, TiradoRives J, Development and testing of the OPLS all-atom force field on conformational energetics and properties of organic liquids, *J Am Chem Soc* **118**:11225−11236, 1996.
25. Halgren TA, Merck molecular force field 2. MMFF94 van der Waals and electrostatic parameters for intermolecular interactions, *J Comput Chem* **17**:520−552, 1996.
26. da Silva J, Dardenne LE, Savino W, Caffarena ER, Analysis of $\alpha4\beta1$ integrin specific antagonists binding modes: Structural insights by molecular docking, molecular dynamics and linear interaction energy method for free energy calculations, *J Braz Chem Soc* **21**:546−555, 2010.

27. Hess B, Kutzner C, van der Spoel D, Lindhal E, GROMACS 4: Algorithms for highly efficient, load-balanced, and scalable molecular simulation, *J Chem Theory Comput* **3**:435−447, 2008.
28. Trott O, Olson AJ, Software news and update autodock vina: Improving the speed and accuracy of docking with a new scoring function, efficient optimization, and multithreading, *J Comput Chem* **31**:455−461, 2010.
29. Morris GM, Goodsell DS, Huey R, Olson AJ, Distributed automated docking of flexible ligands to proteins: Parallel applications of autodock 2.4, *J Comput Aided Mol Des* **10**:293−304, 2004.
30. Newham P, Humphries MJ, Integrin adhesion receptors: Structure, function and implications for biomedicine, *Mol Med Today* **2**:304−313, 1996.
31. Humphries MJ, Integrin structure, *Biochem Soc Trans* **28**:311−340, 2000.
32. Springer TA, Predicted and experimental structures of integrins and beta-propellers, *Curr Opin Struct Biol* **12**:802−813, 2002.
33. Marinelli L, Gottschalk KE, Meyer A, Novellino E, Kessler H, Human integrin alpha v beta 5: Homology modeling and ligand binding, *J Med Chem* **47**:4166−4177, 2004.
34. Jorgensen WL, Chandrasekhar J, Madura JD, Impey RW, Klein ML, Comparison of simple potential functions for simulating liquid water, *J Chem Phys* **79**:926−935, 1983.
35. Zwanzig RW, High-temperature equation of state by a perturbation method — Part 1: Nonpolar gases, *J Chem Phys* **22**:1420−1426, 1954.